Supporting Information

Atomistic Conversion Reaction Mechanism of WO_3 in Secondary Ion Batteries of Li, Na, and Ca

Yang He[+], Meng Gu[+], Haiyan Xiao, Langli Luo, Yuyan Shao, Fei Gao,* Yingge Du,* Scott X. Mao,* and Chongmin Wang*

anie_201601542_sm_miscellaneous_information.pdf
anie_201601542_sm_movie_1.avi
anie_201601542_sm_movie_2.avi
anie_201601542_sm_movie_3.avi

Supporting Information Include:

Supporting Movies 1-3

Supporting Figures S1-S3 and Discussions

Experimental and *Ab* initio Molecular Dynamic Simulation Methods

References

1: Supporting Online Movies

Movie 1: *In situ* TEM bright field imaging of lithiation of WO_3 film

Movie 2: NBD line scan across the reaction front

Movie 3: *In situ* HRTEM imaging of sodiation of WO_3 film

2: Supporting Figures S1-S3 and Discussions

Discussion on the beam effect

As a result of the congruent contraction and distortion of local W-framework, amorphous W were formed. The HRTEM images of the fully lithiated phase (Fig. S1a) show no crystal feature. The diffused diffraction pattern (Fig. S1b) is consistent with the broad peaks in simulated diffraction of polycrystalline W metal with 3 Å grain size. Since the unit cell of body-center cubic W metal is ~3 Å, this means that the W atoms contracted to unit-cell scale clusters with short range order of pure W amorphous structure. On the other hand, radiating with high intensity (300 keV, $\phi \sim 6 \times 10^{19} \ e \cdot cm^{-2} s^{-1}$) electron beam, the amorphous structure gradually transformed into W nanocrystals (Fig. S1c); meanwhile the diffractions from Li_2O became weak. The diffraction pattern of the radiated region (Fig. S1d) shows sharp rings with diffraction spots, which match with the simulated diffraction of polycrystalline W metal with 3 nm grainsize as circled in Figure S1c. This observation indicates that the original amorphous W metal transformed to nanocrystals, which can be primarily attributed to the electron beam induced atom diffusion via heating and atom displacement.[1] Besides, the weakening of Li_2O diffraction can be attributed to electron beam sputtering effect which gradually removes the light atoms from the final phases. Note that the annealed W crystals show obvious texture (Fig. S1d); this may be resulted from the effect of residual intercalation phase on the W crystal growth.

The microstructure of the final phase, especially the length-scale of transition metal clusters (or crystals) is critical to the reversible reaction. Many *in situ* TEM studies on conversion electrodes claimed that transition metal atoms form 1~2 nm nanocrystals after charging,[2] contradicting to the "pseudo-amorphous" structures observed by other techniques.[3] Based on our results, in the initial full-conversion phase, the transition metal clusters should be in angstrom scale, i.e. amorphous state; and annealing factors such as beam induced heating and atom displacement can considerably increase the size of these orders to nanometer scale. It is worth noting that room temperature aging and the heat generated in a working battery may also contribute to the crystal growth in the final phase, especially when lighter atoms (such as Fe, Co, Cu) are involved. Therefore, we can only conclude that the "amorphous" final phase should exist, at least, right after the conversion reaction.
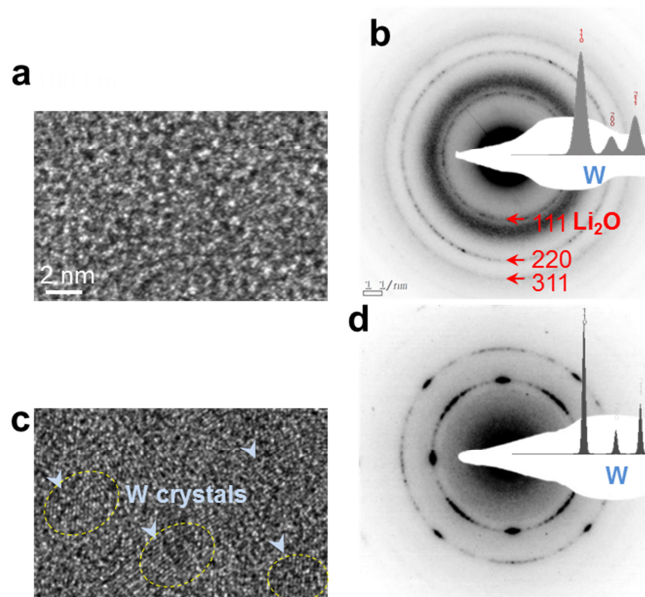
Figure S1, TEM, high resolution TEM and electron diffraction patterns of fully converted phase (a-b) and beam annealed phase (c-d). Insets in (b) and (d) are simulated diffraction intensity profiles of polycrystalline W. The circles and arrows in (c) indicate the W nanocrystals formed after intense electron beam irradiation.
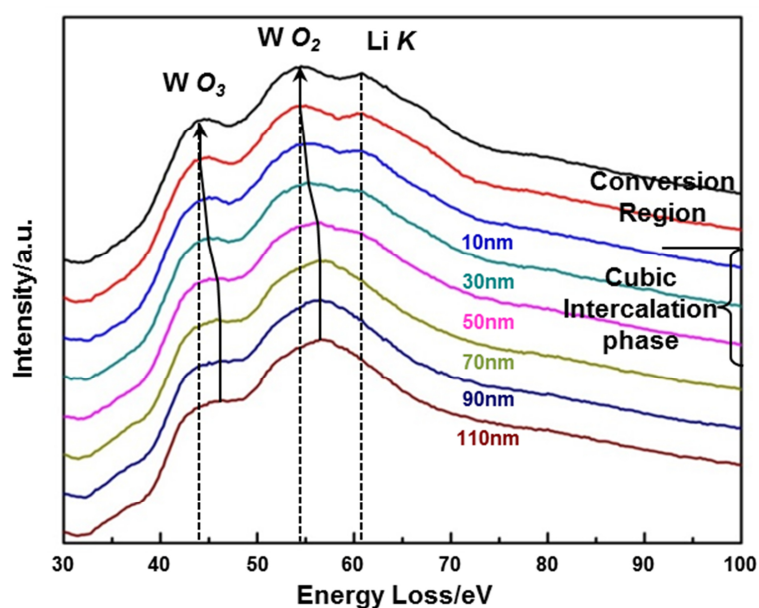

Figure S2, EELS spectrums across the CF in Figure 2a. Black arrows indicate the chemical shift of the W $O_{2,3}$-edges. Note that the EELS spectrums were aligned using zero-loss peak.

Discussion of the intercalation to conversion transition

It is known that pure WO_3 is semiconductor with 2.8 eV bandgap. The group I metals can occupy the A sites in the WO_3, where the group I metal oxides and donates one electron to the

conduction band of WO_3.[4] Researchers also found that following lithium intercalation, Li_xWO_3 becomes metallic when $x>0.25$.[5] Therefore, the intercalation induced semiconductor-to-metal transition, which can enhance insertion rate of Li ions and consequently accelerate subsequent conversion reaction. This catalyzing intercalation region before conversion reaction is directly observed using *in situ* TEM analysis.

With increasing Li insertion, the W framework gradually contracted and distorted. Note that *in situ* NBD imaging of the dynamic evolution of the same local area during Li insertion gave the same results, except for a final phase structure with coarse-grain crystalline W which was likely resulted from electron beam effect (Supporting Figure S1). Since the volume expansion right before conversion started was relatively small (~3% measured at CF Figure 1c), this solid state amorphization might be attributed to the chemical disorders created by excessive Li insertion.

To provide clear insights into the structural changes caused by lithium insertion, *ab* initio molecular dynamics simulations were performed on a transitional stage when 2 Li atoms were injected into each WO_3 unit cell- one at body-center sites and the other at face-center sites of the unit cell. The system was completely relaxed until it reaches a thermal equilibrium state. Supporting Figure S3b and c show the relaxed atomic arrangement and corresponding radial distribution functions (RDF) of the system. It is noted that <W-W> peaks appear around 2.7 Å, which is approximately the nearest bonding distance of 2.74 Å in W metal, indicative of the shrink of W framework to W metal ordering. We also find that <Li-O> bonds are formed in this modeling, as indicated by the appearance of <Li-O> peaks around 2.0 Å, which is comparable to the Li-O bonding distance of 2.00 Å in Li_2O. The distorted lattice structure and contraction of W framework towards W metal ordering derived from our atomistic simulation vividly confirmed the formation of Li_2O and W after final reaction as proved by our NBD observation.

Reviewing above findings, the whole picture of the conversion reaction upon Li^+ insertion into WO_3 electrodes can be summarized as follows. The Li^+ ions diffused along the vacant ⟨001⟩ channels of the lattice, intercalated into the WO_3 unit cells and partially reduced W^{6+}. The intercalation phase gradually evolved from monoclinic to cubic structure with increasing lithium concentration. The increased conductivity effectively facilitated subsequent conversion reaction. Beyond intercalation concentration, Li atoms bonded with oxygen atoms, further reduced W^{n+} and destabilized the W framework which gradually shrunk and distort. At full lithiation, the W^{n+} ions were fully reduced to W^0; the W framework collapsed into amorphous W metal; and Li-O bonds were established to form Li_2O structure.
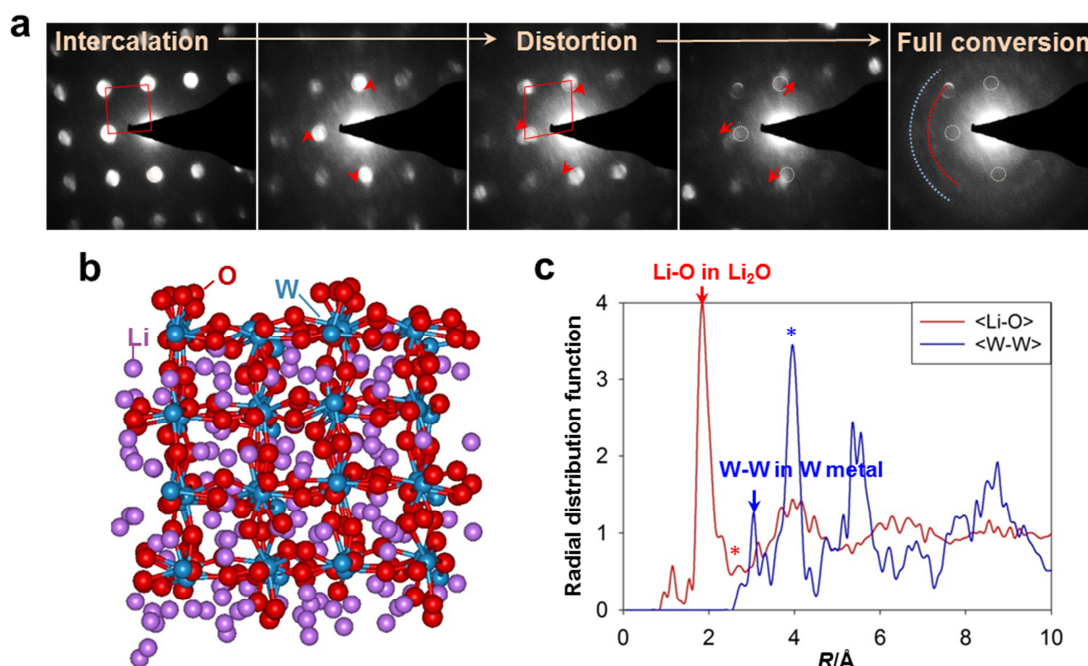
Figure S3, (a) Spatial resolved NBD patterns showing gradual transition from intercalation to full conversion. Arrows indicate shift of diffraction spots with respect to that of original WO_3. (b) Schematic view of the relaxed structure of WO_3 with 2 Li atom-per-unit cell injection, (c) RDFs for <Li-O> and <W-W> in the relaxed structure. Stars indicate shortest <Li-O> and <W-W> distances in the cubic intercalation phase.

Experimental and *Ab* initio Molecular Dynamic Simulation Methods

The TEM sample was made as follows. Together with Nb-STO, the WO_3 film was cut by diamond saw, mechanical polished and Ar-ion milled at 5-2 keV for thin cross-section. Then the cross-section sample was pasted onto Mo ring and loaded on sample side of the Nanofactory-STM holder. Pure metals (Li, Na, and Ca) were loaded onto a tungsten tip and fixed to piezo-system in the Nanofactory holder. This process was carried out in an Ar filled glove box and the whole setup was transferred to TEM via a home-made vacuum container. The total air-exposure time was controlled to be <5 seconds. A thin layer of oxides formed on the metal sources surface working as solid electrolytes. FEI Titan 80-300 S/TEM with probe C_s corrector and ETEM with imaging C_s corrector (both operating at 300 kV) were used for this research. The sample was adjusted to [010] zone axis before experiment. Ion source was navigated to contact the WO_3 film then a constant bias (-0.8 V) was applied between the WO_3 electrode and the ion source (Li, Na or Ca metal) to drive the electrochemical reaction. Counting in the internal electron resistance of the test circuit, the actual overpotential on the WO_3 electrode (vs. Li/Li$^+$) should be lower than 0.8 V. The current during ion insertion was several nano-Ampere, corresponding to a current density of ~10 A/cm^2.

The NBDs and EELSs were taken right after reaction without taking the sample out of TEM. The NBDs were captured with a charge-coupled device (CCD) at 300 kV microprobe scan mode with 50 μm condenser apertures (C2). The probe diameter was measured to be ~3 nm (full width at

half maximum) with 0.9 mrad convergence angle. The EELS spectrums were recorded on the same line as in NBD, at an energy resolution of ~0.8 eV.

The *ab initio* molecular dynamics (MD) simulations were carried out using SIESTA code,[6] based on density-functional theory with the generalized gradient approximation and the Perdew–Burke–Ernzerhof functional. The valence wavefunctions were expanded in a basis set of localized atomic orbitals and double-ζ basis sets were used. In the simulation, a cutoff energy of 150 Ry for the basis set and a Γ-point sampling in the Brillouin zone were employed. The calculations were conducted with a supercell method at constant particle number and volume with periodic boundary conditions imposed along three directions. The supercell consists of 64 W, 192 O atoms, and 128 Li atoms being initially inserted into the body-centered and face-centered sites of the WO_3 unit cell. *Ab initio* MD calculations were then performed to completely relax the whole system until it reached an equilibrium state at 300 K. The simulation time is 3 ps and the employed time step is 1 fs.

References

[1]   R. F. Egerton, P. Li, M. Malac, *Micron* 2004, *35*, 399-409.

[2]   aL. Luo, J. Wu, J. Xu, V. P. Dravid, *ACS Nano* 2014, *8*, 11560-11566; bF. Wang, R. Robert, N. A. Chernova, N. Pereira, F. Omenya, F. Badway, X. Hua, M. Ruotolo, R. Zhang, L. Wu, V. Volkov, D. Su, B. Key, M. S. Whittingham, C. P. Grey, G. G. Amatucci, Y. Zhu, J. Graetz, *Journal of the American Chemical Society* 2011, *133*, 18828-18836.

[3]   aL. Luo, J. Wu, J. Xu, V. P. Dravid, *ACS Nano* 2014, *8*, 11560-11566; bP. Poizot, S. Laruelle, S. Grugeon, L. Dupont, J.-M. Tarascon, *Nature* 2000, *407*, 496-499; cK. E. Gregorczyk, Y. Liu, J. P. Sullivan, G. W. Rubloff, *ACS Nano* 2013, *7*, 6354-6360.

[4]   aS. M. Whittingham, *Teaching General Chemistry: A Materials Science Companion*, American Chemical Society, 1993; bW. Qiang, W. Zhenhai, J. Yeonseok, C. Jiyoung, L. Kwangyeol, L. Jinghong, *Nanotechnology* 2006, *17*, 3116.

[5]   P. M. S. Monk, R. J. Mortimer, D. R. Rosseinsky, *Electrochromism and Electrochromic Devices*, Cambridge University Press, Cambridge, 2007.

[6]   J. M. Soler, E. Artacho, J. D. Gale, A. Garcia, J. Junquera, P. Ordejon, P. D. Sanchez, *J. Phys.: Condens. Matter.* 2002, *14*, 2745-2779.